Spatial patterns of suspended sediment yields in a humid tropical watershed in Costa Rica

Jagdish Krishnaswamy,* Daniel D. Richter, Patrick N. Halpin and Michael S. Hofmockel

Nicholas School of the Environment, Duke University, Durham, NC 27708, USA

Abstract:

Humid tropical regions are often characterized by extreme variability of fluvial processes. The Rio Terraba drains the largest river basin, covering 4767 km^2, in Costa Rica. Mean annual rainfall is $3139 \pm 419_{sd}$ mm and mean annual discharge is $2168 \pm 492_{sd}$ mm (1971–88). Loss of forest cover, high rainfall erosivity and geomorphologic instability all have led to considerable degradation of soil and water resources at local to basin scales. Parametric and non-parametric statistical methods were used to estimate sediment yields.

In the Terraba basin, sediment yields per unit area increase from the headwaters to the basin mouth, and the trend is generally robust towards choice of methods (parametric and LOESS) used. This is in contrast to a general view that deposition typically exceeds sediment delivery with increase in basin size. The specific sediment yield increases from $112 \pm 11.4_{sd}$ t km^{-2} year^{-1} (at 317·9 km^2 on a major headwater tributary) to $404 \pm 141.7_{sd}$ t km^{-2} year^{-1} (at 4766·7 km^2) at the basin mouth (1971–92). The analyses of relationships between sediment yields and basin parameters for the Terraba sub-basins and for a total of 29 basins all over Costa Rica indicate a strong land use effect related to intensive agriculture besides hydro-climatology. The best explanation for the observed pattern in the Terraba basin is a combined spatial pattern of land use and rainfall erosivity. These were integrated in a soil erosion index that is related to the observed patterns of sediment yield. Estimated sediment delivery ratios increase with basin area. Intensive agriculture in lower-lying alluvial fans exposed to highly erosive rainfall contributes a large part of the sediment load. The higher elevation regions, although steep in slope, largely remain under forest, pasture, or tree-crops. High rainfall erosivity (>7400 MJ mm ha^{-1} h^{-1} year^{-1}) is associated with land uses that provide inadequate soil protection. It is also associated with steep, unstable slopes near the basin mouth.

Improvements in land use and soil management in the lower-lying regions exposed to highly erosive rainfall are recommended, and are especially important to basins in which sediment delivery ratio increases downstream with increasing basin area. Copyright © 2001 John Wiley & Sons, Ltd.

KEY WORDS   specific sediment yield; tropical watersheds; rainfall; erosivity; slope; land use; Terraba basin; Costa Rica

INTRODUCTION

The hydrologic response of catchments is controlled by a complex function of ecological, climatic, and geomorphic processes. Scale and heterogeneity in hydrologic processes need to be addressed within a rigorous mechanistic–statistical framework (Sivapalan and Kalma, 1995).

In the humid tropics, two factors combine to limit a quantitative expression of hydrologic and sedimentation response to land-use change. First, fluvial regimes of tropical basins, especially those in the humid tropics, are highly dynamic due to particularly high intra- and inter-annual variability. Second, few tropical catchments of any size are gauged adequately to address within-basin variability or have data available for time scales of decades or more (Bruijnzeel, 1993). Adequate spatially distributed data on rainfall, flow, sediment, land use, topography, and other surface characteristics are essential to evaluate the effects of land use on hydrology.

---

* Correspondence to: Jagdish Krishnaswamy, Ashoka Trust for Research in Ecology and the Environment (ATREE), Post Box 2402, Farm Post Hebbal, Bangalore 560024, India. E-mail: jagdish@atree.org

The lack of data in a highly variable system limits our ability to understand many hydrologic systems in the tropics (Bruijnzeel, 1990).

Until recently, the majority of basin studies that have addressed scale effects on sedimentation have emphasized the decreasing of specific sediment yield with increasing area as one proceeds downstream (Wolman and Schick, 1967; Walling, 1983; Jansson, 1988). This was often assumed to be widely applicable phenomena and has become a global generalization. This pattern is often quantified by a decrease in sediment delivery ratio with basin size. The general view is that opportunities for deposition increase downstream because of reduced river gradients, slopes, and decreased proportional spatial coverage of localized storms. The conventional model of declining mean annual suspended sediment yield (or sediment delivery ratio) with drainage area is often based on agricultural basins with homogeneous terrain in temperate ecosystems. The global validity of this earlier paradigm of decreasing specific sediment yield with size is increasingly being challenged by a growing number of data sets from around the world (Meade, 1982; Ashmore; 1992; Bull *et al.*, 1995; Kithiia, 1997; Bobrovitskaya and Zubkowa, 1998). In many temperate ecosystems the remobilization of previously deposited sediment is known to increase specific sediment yields downstream (Meade, 1982; Ashmore 1992). However, data sets from the humid tropics are rare.

A conceptual analysis of the traditional view was done by Dedkov and Moszherin, (1992). According to Dedkov and Moszherin (1992), river systems will be characterized by either positive or negative relationships between specific sediment yield and catchment area according to the relative importance of channel and slope erosion. Where channel erosion is dominant, as in well-vegetated basins, erosion rates will increase downstream, whereas in regions dominated by slope erosion (sheet and gully) the rates will decrease downstream. This is because most of the erosion will often be concentrated in steeper headwater areas and a proportion of the mobilized sediment will be deposited during transport through the system. Although Dedkov and Moszherin (1992) based their observations on 1872 mountain rivers around the world, rivers from humid tropical basins were almost absent. Most of the basin data examined were from temperate, semi-arid and cold desert regions. In addition, there is inadequate appreciation of the spatial patterns of land use and other basin characteristics, such as rainfall erosivity, that may influence trends in specific sediment yield within a single basin.

This conceptual view may not be widely applicable to many basins, where the upper reaches are generally forested, whereas the middle and lower reaches are under less protective land use, especially in the humid tropics (Sader and Joyce, 1988). The few nested catchment data from the humid tropics that are available suggest that the traditional view is not prevalent (Simon and Guzman-Rios, 1990; Dickinson and Bolton, 1992; Williams, 1995). Detailed spatial analyses of specific sediment yield in relation to hydro-climatology, soils, geomorphology and land use are particularly scarce for tropical humid basins.

The Rio Terraba in Costa Rica is the country's largest river, and drains what may be one of the best-gauged basins of comparable size (5000 km^2) in the humid tropics. Here, data are available from a nested network of eight stations covering sub-basins from 100 to 4767 km^2 for up to three decades. This basin has experienced severe soil and water-quality degradation in recent decades due to the development of extensive and intensive land uses whose patterns can be estimated by remotely sensed data and maps based on aerial photography.

The objectives of this study are to: (1) define the spatial patterns of sediment yield in the Terraba basin in Costa Rica using available hydrologic and sediment data; (2) characterize the downstream patterns of specific sediment yield with respect to the controlling factors of slope, rainfall erosivity and land use using statistical methods and spatial techniques.

STUDY AREA

Geology, landforms and soils

The Terraba River (Figure 1) drains a basin of 4767 km^2 in the southern part of Costa Rica and flows out into the Pacific Ocean. The geology of Costa Rica including the Terraba basin is well described (Castillo-Munoz,
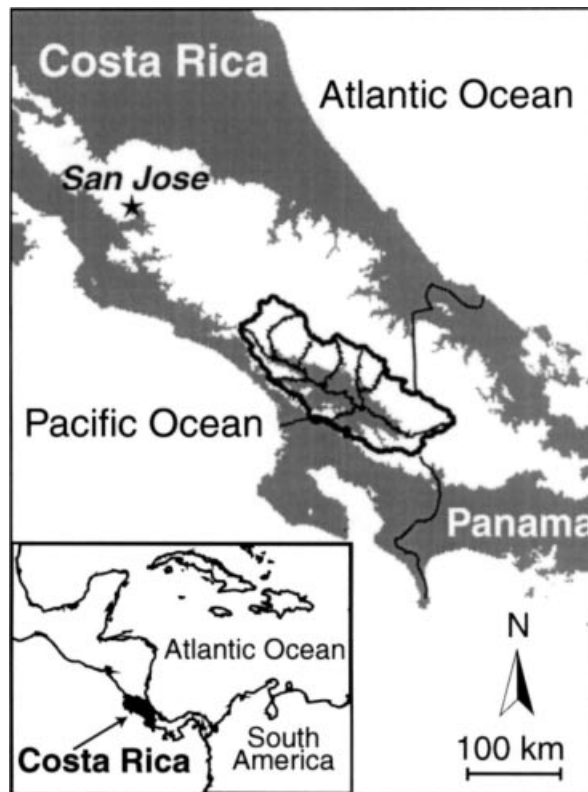
Figure 1. Location of Terraba basin (thinner black line) within Costa Rica (thick black line) with major rivers in the basin marked. The Cordillera Talamanca and the Fila Costena (>300 m msl) are shown in white

1983). It is located in a structural depression (Terraba Trough) that continues into Panama and is bounded by the Fila Costena or Costeda (Coast Range) in the south and the Cordillera de la Talamanca in the north. The maximum elevations of these two ranges are 1300 m (Cerro Canas Gordas) and 3819 m (Mt Chirripo) respectively. It is made up primarily of Tertiary sedimentary rocks, diabase dykes, and volcanic rocks of Upper Tertiary age in the central part.

The Coast Range (Costeda) is composed of Cretaceous to Quaternary deep-water marine sedimentary rocks. These include sandstones, siltstones, conglomerates, shales and claystones. The Cordillera Talamanca is composed of uplifted Cretaceous marine sedimentary and volcanic rocks with local intrusions of Tertiary quartz diorite, granodiorite, granite and sienite. The sedimentary rocks include rudites, sandstones and claystones. The volcanic rocks are generally andesitic and basaltic in nature with some tuffs and ignimbrites intruded by basalt bodies. These are found to lesser degree in the Talamanca and Costeda mountain ranges. Black shale appears extensively in the General valley and the Costeda Range. At the foot of the Cordillera there are fans and terraces on colluvial–alluvial materials of Pleistocene origin derived from the Cordillera that are drained by braided networks of streams. The steep slopes give way to these fan surfaces at about 1000 m elevation. These occupy about 400 km^2 of the basin and are now under intensive agriculture and pasture. Bauxite and highly weathered soils are found on these surfaces. Uplift of the two bounding mountain ranges relative to the incising streams cause the higher abandoned terraces to have the oldest soils (Kesel and Spicer, 1985).

The highlands are characterized by steep slopes, and about 70% of the area above 300 m has >30% slope. The Rio General and Rio Coto Brus drain the western and eastern portions of the valley, respectively and

1. Palmar on Rio Terraba
2. El Brojo on Rio General
3. Remolino on Rio General
4. La Cuesta on Rio General
5. Caracucho on Rio Coto Brus
6. Las Juntas on Rio Pacuar
7. Rivas on Rio Chirripo
8. Pejibaye on Rio Pejibaye
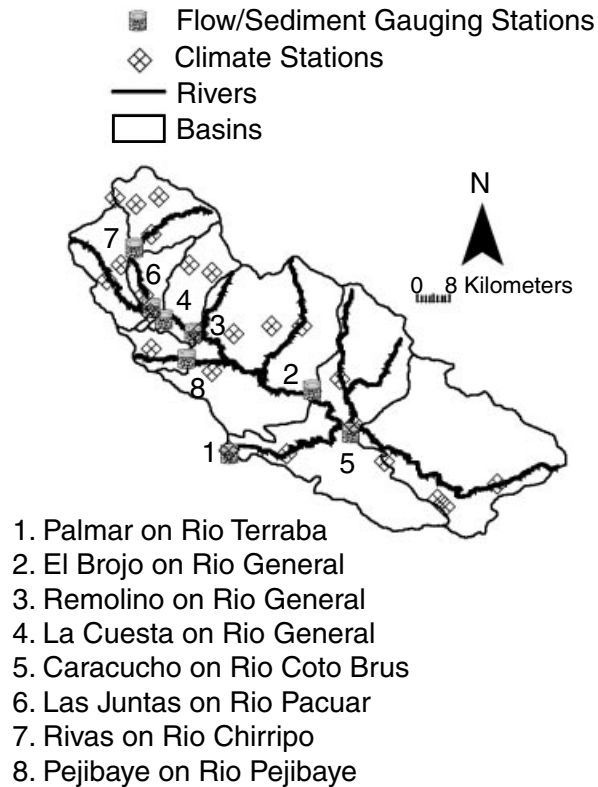
Figure 2. Location of long-term meteorological gauging and sediment sampling stations in the Terraba basin. There are eight stations for flow and sediment, 22 for rainfall and five for pan evaporation in all. Elevation is based on 1 km digital data

combine to form the Rio Terraba (Figure 2). The stream and river beds materials are generally coarse, ranging widely in size from large boulders (>1 m diameter) to sand.

Soil characteristics, like that of geology, are correlated with landscape position and topography. The soils in the basin range from Entisols and Inceptisols on recent alluvium, Histosols on localized seasonally flooded lacustrine margins, Alfisols, Ultisols and Oxisols on older, stable river terraces and fans, Andisols on ash deposits, and Inceptisols in the highland soils, some subjected to recent glaciation (Kesel and Spicer, 1985; MAG, 1991). In general, soils under protective vegetation are considered resistant to erosion and have rapid vertical drainage. However, the intense rainfall and forest conversion to cultivation and pastures make them vulnerable to run-off and erosion.

Costa Rica is seismically very active. Moderate and major earthquakes have caused extensive immediate and post-event surface damage in parts of the Terraba basin. This is mainly through liquefaction and landslide activity during subsequent intense rain events causing high rates of sediment generation (Mora, 1989).

Climate and hydrology

The annual rainfall in the basin ranges from below 1500 mm to over 7000 mm and displays strong spatial, elevation and seasonal effects. The basin-wide rainfall averages $3139 \pm 419_{sd}$ mm year^{-1} based on 22 rain gauges operating between 1971 and 1988. The dry season (January–April) ranges spatially from 1 to 5 months, with 0–100 mm rainfall per month. In the wet season (May–December) there is often a short drier period in June–July. In October, the wettest month, rainfall can exceed 1000 mm. The average annual pan evaporation

is about $1233 \pm 71_{sd}$ mm, with a maximum of over 160 mm in March ($n = 5$ stations, 1971–88 hydrologic years). The annual flow of the Rio Grande de Terraba, Costa Rica's largest river, at the basin outlet (station at Palmar) for the period 1971–88 is $2168 \pm 492_{sd}$ mm. The flow coefficient is therefore over 60% of annual rainfall.

Vegetation

The Terraba basin has a wide range of natural ecosystems, a consequence of the diversity of geology, elevation, soil, landform and climate. Soto and Gomez (1993) categorize these into 17 types, ranging from lowland tropical humid forests to tropical boreal paramo with stunted shrub vegetation in the highest elevations (>3000 m). Areas with a longer dry season and ustic soil moisture regime have savannah–woodland ecosystems with scattered fire-tolerant trees and shrubs. The origin of these can be attributed to a combination of longer dry-season, frequent fire and prior land use (Boucher *et al*., 1983; Kesel and Spicer, 1985).

Land use

Deforestation and human activities have substantially modified the vegetative cover of the basin. Except for protected areas, such as the La Amistad Biosphere Reserve at high elevation, 80% of the forests have been converted to pasture. The La Amistad Biosphere covers 6126 km^2, straddling the Talamancas on both sides of the ridge, including a core national park area of 1939 km^2. The protected area on the Pacific side of the ridge lies within the upper elevations of the Terraba basin.

The land under forest cover declined from over 60% in the early 1970s to about 40% in the late 1980s to early 1990s. An estimated 1954 km^2, or about 41% of the total basin area, was covered by pasture by the early 1980s. Pineapple, sugar cane, coffee, corn, beans, and a variety of other crops and horticulture account for the rest of area. Below La Amistad and other protected areas, only small patches of forest (<10 km^2) remain intact. These serve as a reminder of the magnificent lowland forests that covered the basin barely half a century ago (Skutch, 1971).

DATA

Fluvial transport and hydrology

A dam on the Rio Terraba was first proposed in the early 1960s, and, as a consequence, high-quality meteorological, hydrologic and sediment data in the Terraba basin are relatively abundant. Monthly rainfall data for stations in the basin (Figure 2), collected by ICE, Costa Rica's national hydroelectric authority, and IMN, the National Meteorological Institute of Costa Rica, were obtained from published bulletins (IMN, 1988; ICE, 1994a).

Fluvial data were obtained from ICE (1994b), which operates the network of monitoring stations in the Terraba basin. Daily mean flow data, in cubic metres per second, for the eight gauging stations (Figure 2) covering the period 1971–93 were available from stations gauging flow from catchments that ranged from 128 to 4767 km^2.

Suspended sediment concentration data, measured by depth-integrated sampling, followed by evaporation and gravimetric analyses were assembled for all eight stations. These data were generally monthly, but also included some intensively sampled storm events at each station. The original data set included instantaneous discharge corresponding to the sediment sampling (Table I). This data set comprises 2205 observations for all eight stations, including 46 observations exceeding 1000 mg l^{-1}. The sediment sampling covered a wide range of flow conditions and sediment concentrations (Table I).

All storm events were averaged to a single daily concentration corresponding to the mean daily flow. This derived data set is the main focus of this study. The sediment data set corresponding to the daily flow records ranged between 242 and 301 samples per station for the period 1970–93. In addition, for a few stations, data

Table I. Details of instantaneous discharge and corresponding sediment sampling:
1970 to 1994

Station	Max. flow sampled (m^3 s^{-1})	Sediment concentration (mg l^{-1})		
		95% quantile	99% quantile	Maximum
Pejibaye	44·9	65·5	141·94	465
Rivas	119	91	265·32	5187
Las Juntas	237	241·35	1696·41	3243
La Cuesta	272	123·5	1195·78	2465
Remolino	469	207·4	573·08	1193
Caracucho	686	284·4	821·92	2088
El Brujo	1042	370	1201·5	1889
Palmar	2340	511·2	1393·24	3006

on sediment concentrations and corresponding instantaneous discharge were available up to 1994, but the daily flow records available were only up to April 1993. However, for this study, only the 1970–93 data were considered for the main sediment yield estimates, although two different estimates based on the instantaneous discharge and corresponding instantaneous sediment concentrations and discharge are also presented.

The distribution of the daily flows that were actually sampled for sediment in relation to the distribution of the full range of continuous daily flow needs to be considered. This is particularly important where a few high flows transport a large amount of sediment. The comparison of the daily flows actually sampled to the larger continuous daily flow data sets (Table II) indicates that the sediment sampling was generally adequate to capture a wide range of daily mean flow conditions.

To examine suspended sediment transport in the basin in greater detail, ICE data were supplemented by intensive sampling by the authors in the wet-season of 1995. Suspended sediment samples ($n = 109$) were collected at eight locations corresponding to mixed land-use sub-basins (28 to 318 km^2) using grab and DH-59 sampling (Guy and Norman, 1970). Suspended sediment samples were analysed for sediment concentration and turbidity in addition to other water-quality parameters. Additional details of site, sampling, and methods are described elsewhere (Pachon, 1996; Krishnaswamy, 1999).

METHODS

Sediment rating models

Linear regression models were used to generate transformed sediment rating curves:

$$\text{SEDC} = A(\text{FLOW})^B \tag{1}$$

$$\log_{10}(\text{SEDC}) = A + B\log_{10}(\text{FLOW}) + \varepsilon \tag{2}$$

where SEDC (mg l^{-1}) is the suspended sediment concentration, FLOW (m^3 s^{-1}) is the daily mean flow, A is the intercept or constant, B is the slope coefficient, and ε is the residual error $\sim N(0, \sigma^2)$.

Even though sediment sampling was usually monthly, the sediment transport estimates for a particular day based on a rating curve are often statistically well defined compared with a single measurement on that day. This is because though daily observations are subject to the sampling error of a single observation, the model estimates for a day are based on the entire data set (Clarke, 1990; Cohn et al., 1992; Parker and Troutman, 1989). The intermittent nature of sediment sampling avoids or reduces the serial correlation that more frequent sampling may exhibit (Clarke, 1990). This minimizes problems with violation of independence assumptions in the linear model.

Table II. Comparison of flow characteristics of sediment sampling in relation to all daily gauged flows at each station

Station	River	Area (km^2)	Median	75% (3rd quartile)	95%	99.73% (1 year flow)	Maximum
Pejibaye	**Pejibaye**	128					
complete daily flow record ($m^3 \ s^{-1}$)			2·84	6·81	20·9	**89**	393
daily flows sampled for sediment			3	6·61	20·66		47·4
Rivas	**Chirripo**	318					
complete daily flow record ($m^3 \ s^{-1}$)			17·4	29·9	56·4	**111**	354
daily flows sampled for sediment			17·3	28	49·06		76·1
Las Juntas	**Pacuar**	322					
complete daily flow record ($m^3 \ s^{-1}$)			14·6	29·2	61·3	**146**	570
daily flows sampled for sediment			15·1	29·2	58·7		179
Caracucho	**Coto Brus**	1133					
complete daily flow record ($m^3 \ s^{-1}$)			50·6	95·43	204	**382**	1139
daily flows sampled for sediment			54·4	105·2	202·2		290
La Cuesta	**General**	835·5					
complete daily flow record ($m^3 \ s^{-1}$)			48	86·22	165	**344**	1377
daily flows sampled for sediment			51·25	85·48	152·85		244
Remolino	**General**	1076					
complete daily flow record ($m^3 \ s^{-1}$)			64·2	113·0	204	**401**	1580
daily flows sampled for sediment			65·1	111·2	202·2		577
El Brujo	**General**	2401					
complete daily flow record ($m^3 \ s^{-1}$)			116	233	490	**1069**	4533
daily flows sampled for sediment			109	203	430		1550
Palmar	**Terraba**	4767					
complete daily flow record ($m^3 \ s^{-1}$)			228	444	869	**1909**	6148
daily flows sampled for sediment			253	498	490		2520

The range of sediment concentrations observed during the 1995 wet-season intensive storm sampling (95% quantile: 2286 mg l^{-1}; max: 4643 mg l^{-1}) are comparable to the sediment data sets from the long-term ICE stations described above (also see Figure 3 and Table I). This suggests that the ICE sampling regime is generally representative of the range of sediment concentrations expected in the Terraba basin. We conclude that the regression models based on the sediment sampling at the eight long-term gauging stations used in this study did not substantially underestimate sediment concentrations at high flows.

Based on the regressions, the linear approximation is considered a valid representation of the range of the discharges that were sampled for all the eight stations (Figure 3). Graphical diagnostic techniques were used to check for serious violations of assumptions, such as normality and heteroscedasticity. The models seem to be a reasonable compromise between fluvial reality and statistical validity on the one hand and data constraints on the other hand.

The regression models were used to predict daily sediment concentrations using the flow time-series. The retransformed sediment concentration is:

$$SEDC' = 10^{(A+B \ \log_{10}(FLOW))} \ \exp(2·65 \ s^2)$$

(3)

where σ^2, the unknown population variance, is substituted by s^2, the square of the standard residual error of the regression model. The correction factor $\exp(2·65 \ s^2)$ compensates for retransformation bias (from the $\log_{10}$−linear to linear) and is recommended for sediment rating curves (Ferguson, 1986; Koch and Smillie, 1986). The mean daily flow and corrected sediment concentration estimate were combined to yield daily and annual transport and yield estimates.
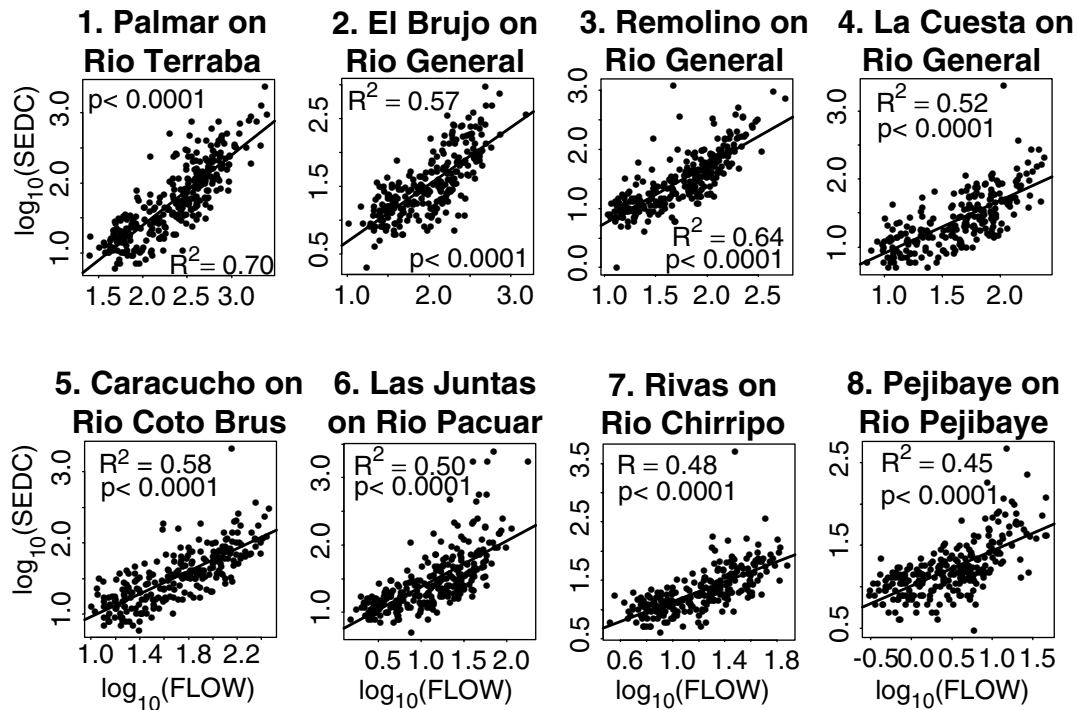
Figure 3. Linear models fit to log-transformed sediment concentration (SEDC) and flow (FLOW) at eight stations. The units of measurement for flow and sediment concentration are m^3 s^{-1} and mg l^{-1} respectively. The numbers 1 to 8 refer to station numbers marked in Figure 2

The estimated sediment yields are representative of the basin conditions because the sediment rating equations were applied to the daily flow records over the same time period corresponding to the collection of sediment samples (1971–93). The data contributing to the models covered a wide range of flow conditions and inter-annual variability.

The rating equation is a simplification of a more complicated process, and uncertainty should be addressed in all such estimates. Few studies report the uncertainty of sediment yield estimates based on rating models. In this study, the variance of the total load was estimated as follows:

$$\text{Load} = \sum_n 0{\cdot}0864\ \text{FLOW}_i (10^{\beta_j X_i + \varepsilon_i}) \tag{4}$$

$$\text{Var(Load)} = 0{\cdot}0864 \left(\sigma^2 \sum_n F_i^2 + \left(\sum_n F_i X_i \right)' \exp \left(\sum_n F_i X_i \right) \right) \tag{5}$$

where F_i is the daily flow treated as a constant, X_i is the daily flow as a variable, β_j is the regression coefficient matrix, ε_i is the error, $(\Sigma_n F_i X_i)$ is the linear model parameter covariance matrix, and Σ_n is the summation over n days in the record. The bias correction was applied to these bounds as well (Ferguson, 1986).

The linear model, as defined earlier, assumes that a single relationship exists between $\log_{10}$ (flow) and $\log_{10}$ (sediment concentration) and is independent of magnitude of discharge. Although the transformation is sometimes adequate to address the non-linearity in the original scale, persistence of post-flow-based response in transformed space may remain. In order to account for these potential problems, and to compare results, alternative methods can be used. A robust iterative local regression model, LOESS (Cleveland, 1979; Cleveland

and Devlin, 1988), was used to fit a locally fitted polynomial (Figure 4). A disadvantage is that the LOESS model cannot predict sediment concentrations for flows beyond the range of flows used to fit the local regression model. As a result, no predictions can be made for several very large flows that transported substantial amounts of sediment. Parametric log–linear models can predict for all flows, although they may not be appropriate. The local regression models will, however, be more accurate over the range of the sample data.

Apart from the parametric and LOESS daily mean flow-based estimates, two other types of sediment yield estimate were generated for comparison. The two models discussed above were based on daily mean flow data and were applied to the continuous daily mean flow data. The two methods described below, although widely used, differ in that they are based on fitting models to instantaneous flow and corresponding sediment concentration or discharge, and applied to the continuous daily flow data. The methods described earlier are therefore more appropriate within the regression framework because, as a measure, instantaneous flow is different from daily mean flow. Regression models should, in principle, be used for prediction purposes or applied using data similar to what was used to fit them.

The regression models based on instantaneous discharge and corresponding sediment concentration sampling up to April 1993 are based on a larger range of discharges and sediment concentrations. The sediment yield estimates were obtained in the usual manner by applying the regression models to the continuous daily flow data.

The instantaneous flows and the corresponding individual sediment concentration data (including the storm events) were available beyond April 1993 up to early 1994, although daily flow records were available only up to April 1993. In order to take advantage of these additional data, one more set of sediment yield estimates were generated as a comparison. These estimates were based on the equations available for each station derived by ICE from the sediment-flow data. Non-linear power equations relating sediment discharge in tonnes per day to instantaneous flow Q (aQ^b) were fit piecewise to the data for three flow ranges at each station. This method suffers from the problem that a strong correlation could exist between the independent (water discharge) and dependent (sediment discharge) variables just because of a common shared variable being incorporated in the dependent variable. These were then applied to the corresponding ranges of the continuous daily flow record up to April 1993 to generate sediment yield estimates. Estimates for intermediate sub-basins between nested stations were obtained by mass balance.

The sediment yield estimates based on different methods are presented for comparisons in Table III.
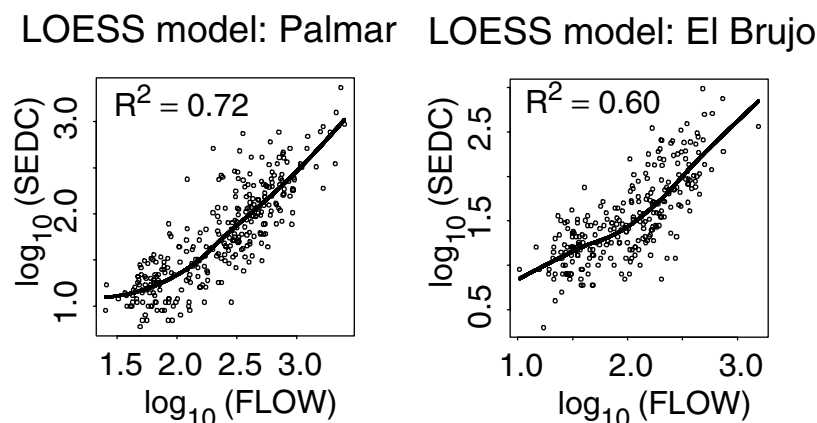
Figure 4. Local regression LOESS models fit to log-transformed sediment concentration and flow data shown as examples for two of the eight stations. Note how the LOESS model is able to account for any flow-magnitude-based changes in slope of the relationship compared with the models in Figure 3

Table III. Characteristics of sub-basins corresponding to gauging stations

Station	River	Elevation[f] (msl)	Area (km²)	Gradient (%)	Slope average (%)	Rainfall annual (mm)	Flow depth (mm)	Sediment yield (t km⁻² year⁻¹)				Land-cover forest (%)
								Daily mean[a]	LOESS[b]	Instantaneous[c]	ICE[d]	
Pejibaye	Pejibaye	395–1103	128	9.4	6.9	2946	1513	62 ± 6·2	43 (114)	63	105	16·9 (9·2)[e]
Rivas	Chirripo	803–3688	318	16	18·6	3585	2200	112 ± 11·4	81 (116)	126	163	44·3 (56·8)[e]
Las Juntas	Pacuar	532–2273	323	3·9	8·74	3587	2165	170 ± 13·4	167 (64)	188	322	15·0 (17·1)[e]
Caracucho	Coto Brus	143–3096	1133	4·9	9·0	2942	1953	154 ± 27·5	121 (101)	222	235	66·9
La Cuesta	General	475–3688	836	0·6	12·25	3563	2370	152 ± 33·9	120 (88)	185	226	27·3
Remolino	General	440–3688	1076	0·62	12·64	3525	2346	222 ± 39·1	200 (61)	239	275	29·9
El Brujo	General	186–3688	2401	0·57	11·13	3256	1882	264 ± 87·6	245 (18)	380	535	27·7
Palmar	Terraba	32–3688	4767	0·28	10·93	3309	2085	404 ± 141·7	332 (28)	438	389	41·3

[a] Estimates of sediment yield based on regressions of daily mean flow and daily mean sediment concentrations. Figures in parentheses are one standard deviation.
[b] Estimates of sediment yield based on LOESS local regression models (1970–93). Numbers in parentheses are number of daily flows beyond range of data used to fit non-parametric model.
[c] Estimates of sediment yield based in regressions using instantaneous flow and sediment concentration data (1970–93).
[d] Estimates of sediment yield from ICE based on piece-wise power equations of sediment discharge and flow (1970–94).
[e] MSS-based land-cover/land-use estimates for these sub-basins were affected by partial non-coverage and/or cloud cover. Alternative estimates based on different techniques (Calvo, 1998) are provided for comparison.
[f] Based on 1 km digital elevation data.

The ICE-based sediment yield estimates for the eight Terraba sub-basins for the water years 1981–87 were combined with data for 21 independent sub-basins in Costa Rica obtained from published sources (Calvo, 1998). This larger data set ($n = 29$), which included data on land use, was used to explore and establish more generic relationships between basin parameters such and sediment yield.

Spatial analyses

The original digital elevation data set was developed by USGS using DTED® Level 0, a product of the National Imagery and Mapping Agency (USGS, 1997). Existing digital elevation data at 3 arc-second spacing (approximately 90 m) were obtained and generalized to the desired 30 arc-second cell size (nominally 1 km) by these institutions. Slope (Figure 5(a)) was derived from the DEM data using a 3×3 window.

Landsat MSS images for 1979, 1986 and 1992 (Krishnaswamy, 1999) classified into pasture, cultivated agriculture and forest, as well the 1 : 200 000 1988 Costa Rica forest map (MIRENEM, 1988), were used to derive a baseline land-cover/land-use map (Figure 5). The land-use map was generated from different sources, primarily because no one source either covered the whole basin or the range of classes required. The areas under intensive agriculture were derived from the MSS supervised classification (65 m pixels), whereas the forest and pasture classes were based on all the sources. This map reflects the approximate land-cover status in the middle of the period of hydrologic records, the early to mid-1980s. The estimates of MSS based land-cover/land-use in the mid-1980s for three of the smaller sub-basins were affected by cloud cover and/or partial or non-coverage. However, use of alternative estimates based on different methods (Table I) taken from other sources (Calvo, 1998) did not change any of the results or conclusions.

Available rainfall data from 60 stations in and around the basin were used to generate an annual rainfall surface map (Figure 6). A fifth-order polynomial equation was used, and this was resampled to a grid of 2·5 km^2 cells. The higher-order polynomial was chosen after comparison with lower-order models in their ability to capture the considerable spatial variability in rainfall in the basin. Comparison with a LOESS surface fit and previously published rainfall map (ICE, 1973) indicated that the polynomial fit was able to incorporate local spatial variations.

Rainfall erosivity

Rainfall in the humid tropics is often characterized by its high erosivity due to its intensity, relatively large drop size and large volume (Lal *et al.*, 1980).
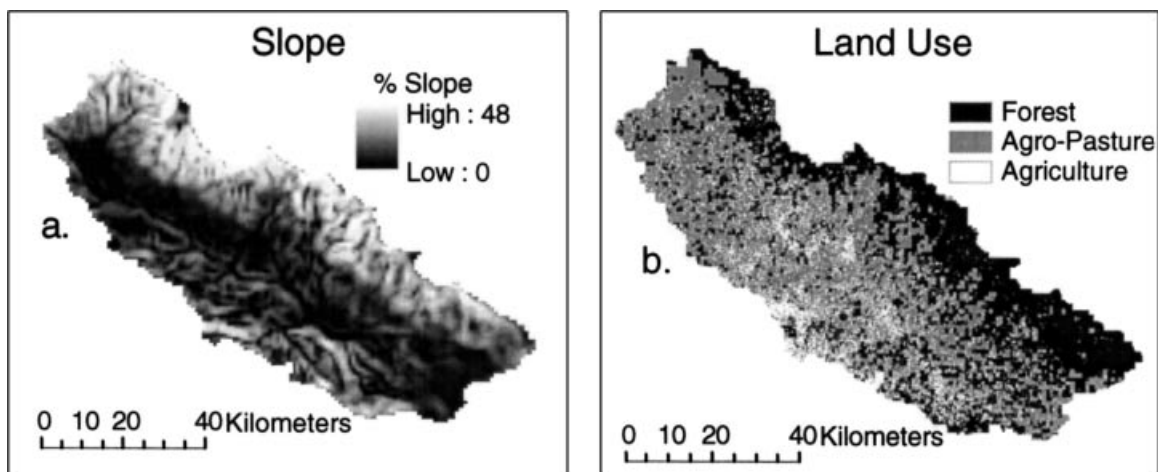
Figure 5. (a) Slope (%) and (b) land-use patterns in the Terraba basin. Slope was derived from 1 km digital elevation data and land use was based on digitally classified Landsat MSS data and published land-cover maps
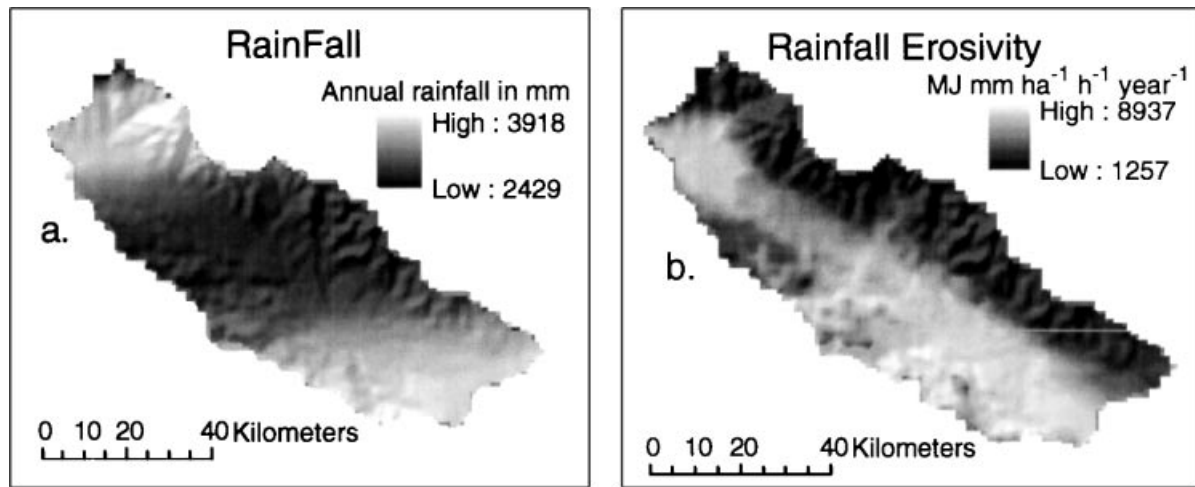
Figure 6. Annual rainfall (a) and rainfall erosivity (b) patterns in the Terraba basin. The rainfall map was based on a polynomial surface fit to average annual rainfall data for 59 stations. Rainfall erosivity was estimated using a regression equation based on annual rainfall and elevation derived for Costa Rica. This regression was run on the available annual rainfall (see above) and elevation (see Figure 2) spatial data

Rainfall erosivity data was generated by using the regression equation: $R = 3786 \cdot 6 + 1 \cdot 5679R - 1 \cdot 9809E$, $n = 111$, $R^2 = 0 \cdot 614$, $p = 0$, predicting annual rainfall erosivity (MJ mm ha^{-1} h^{-1} year^{-1}) from mean annual rainfall R (mm) and elevation E (m), derived for Costa Rica (Vahrson, 1990; Mikhailova *et al.*, 1997). This was applied to the respective GIS data (rainfall and elevation) described earlier. The resultant erosivity map (Figure 6) was resampled to $2 \cdot 5$ km^2 cells.

Erosion indices and sediment delivery ratio

Three of the most important factors determining erosion potential in the humid tropics are slope, land use and rainfall erosivity (Lal, 1977; El-Swaify and Dangler, 1982). Rainfall of very high energy (intensity) and duration on steep, unstable slopes or in association with particular land uses can generate locally high sediment yields in the Terraba basin (Mora, 1989). Two types of erosion index for the basin were derived from the slope, land use and rainfall erosivity GIS data. An approximate land-use erosion factor was assigned to each of the three principal land-use/land-covers: 1 for forest, 100 for pasture and small-scale cultivation, and 1000 for intensive agriculture. This was based on studies in the humid tropics (Sanchez, 1976; El-Swaify and Dangler, 1977, 1982; Dunne, 1979; Dunne and Dietrich, 1982; El-Swaify, 1990). This was combined with slope and rainfall erosivity as follows:

$$\text{EROSION INDEX}_1 = \text{land-use factor} \times \text{rainfall erosivity}$$

$$\text{EROSION INDEX}_2 = \text{land-use factor} \times \text{slope} \times \text{rainfall erosivity}$$

The resultant indices were normalized and expressed on a scale of 1 is to 100.

The main purpose for using these simple indices was to evaluate the relative importance of the principal controls on spatial variability in erosion in the basin. Data based on universal soil loss equation (USLE) erosion estimates for three independent sub-basins (out of a total of eight) within the Terraba basin were available (Calvo, 1998). These were used to calibrate the two erosion indices to actual erosion units of t km^{-2} year^{-1}. Based on the two regressions (index 1, $R^2 = 0 \cdot 99$, $p < 0 \cdot 0002$ and index 2: $R^2 = 0 \cdot 88$, $p < 0 \cdot 06$), predicted erosion estimates were calculated for the sub-basins corresponding to the eight gauging stations (Figure 7).
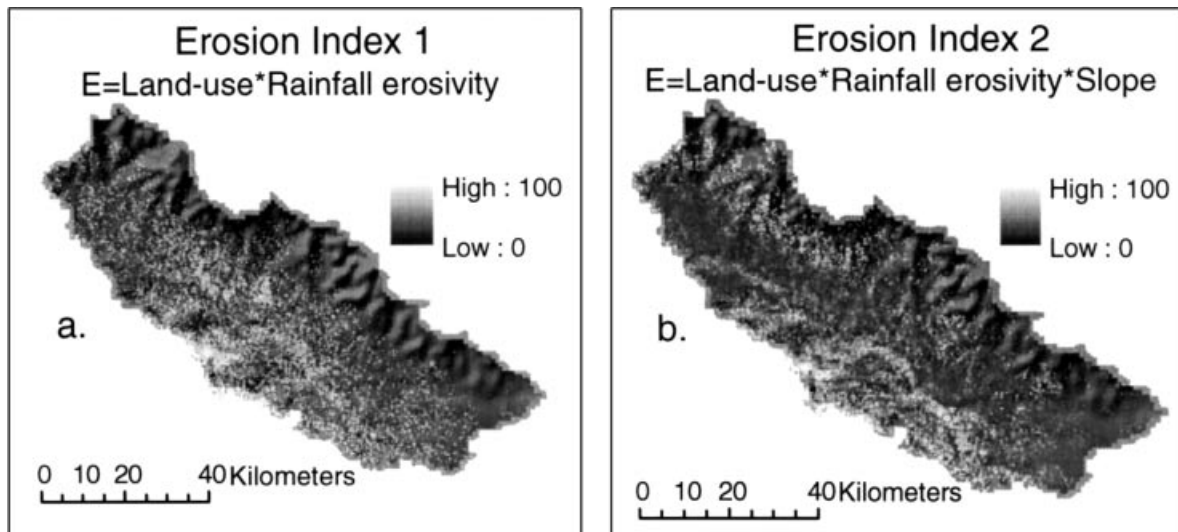
Figure 7. Two simple multiplicative erosion indices generated for the Terraba basin. Index 1 is based on an assumed land-use factor and rainfall erosivity, whereas index 2 incorporates slope in addition to the other two factors

The observed sediment yield at each gauging station divided by the estimated erosion was taken as the sediment delivery ratio. This is considered valid because we assume that most of the suspended sediment is emerging from hill slope erosion. It was observed that, during intensive sediment sampling in 1995 wet season, the sediment peak usually coincided with the discharge peak during storms. This was also observed for the storm events covered by the ICE data sets. In addition, concentrations were lower on the falling limb of the storm hydrograph. All this indicates a strong linkage between rainfall storm related run-off on hill slopes and erosion. There is, however, not enough data or field observations to assess the hill-slope–channel links with much certainty. More field data would be required to get a clear idea of the geomorphic and hydrologic links between the hill slope and channel. The estimates of sediment delivery ratios, as described above, should therefore be considered as an approximate and possibly preliminary attempt until better estimates of erosion are available.

RESULTS AND DISCUSSION

Sediment yield

Parametric and LOESS models. The estimated specific sediment yield at the mouth of the basin at Palmar is $404 \pm 141 \cdot 7_{sd}$ t km^{-2} year^{-1} for a basin area of 4768 km^2. This is the highest specific sediment yield of the eight stations measured (Table III). The lowest yield of the eight stations was $62 \pm 6 \cdot 2_{sd}$ t km^{-2} year^{-1} for Pejibaye, a 128 km^2 basin.

The sediment yield estimates for the areas draining to all the eight stations obtained by the parametric and non-parametric methods were similar (Table III), although the difference increases with basin size. The LOESS model estimates are consistently lower compared with the parametric method, and this is attributed to the missing estimates for flows beyond the range used to fit the non-parametric model. However, the LOESS model is expected to predict more accurately within the range of the sampling data. The maximum difference between the two methods was 19·6% at the basin mouth.

The observed sediment yields in the Terraba basin are comparable to published data from other tropical, mountainous, humid basins in the region. Out of the eight stations, only four (nos 5, 6, 7 and 8 in Figure 2) correspond to independent sub-basins. The estimated specific sediment yields of intervening sub-basins using

the nested data in combination with the four independent station data were $170 \cdot 8 \pm 98 \cdot 39_{sd}$ t km^{-2} year^{-1} for basin sizes below 500 km^2 ($n = 5$) to $508 \cdot 7 \pm 377 \cdot 8_{sd}$ t km^{-2} year^{-1} for three sub-basins larger than 1000 km^2.

An analysis of sediment yield data (1981–87 water years) for 21 independent sub-basins covering a wide range of area (12 to 367 km^2) and land cover (0 to 100% forest) in other parts of Costa Rica (Calvo, 1998) gave a comparable range of yields ($180 \cdot 3 \pm 199 \cdot 42_{sd}$, $88 \cdot 1_{median}$ t km^{-2} year^{-1}). In Puerto Rico, the suspended sediment yield for three forested watersheds ranged from 120 to 525 t km^{-2} year^{-1} depending on geology, whereas it was 746 t km^{-2} year^{-1} for an agricultural watershed with similar geology to the forested watershed with the higher yield (Larsen, 1997).

Influence of basin size and downstream patterns

Along the main Rio General channel the specific sediment yield increases from $152 \pm 33 \cdot 9_{sd}$ t km^2 year^{-1} at La Cuesta (836 km^2) on the Rio General to $404 \pm 141 \cdot 7_{sd}$ t km^{-2} year^{-1} at Palmar on the Rio Terraba at the basin mouth (4767 km^2). The results derived from the LOESS model yields indicate the same pattern (Table I). The pattern observed is therefore not an artifact of applying a log–linear parametric regression model.

Opportunities for erosion increase with basin area over and above any increase in sediment deposition and sediment storage capacity. Moreover, the proportion of estimated total sediment transported in a month, which is a reflection of the 'flashiness' of a watershed, is invariant with basin size (Table IV), and does not decrease as one would expect if the 'buffering' effect of storage and increased deposition were present.

Sediment parameters and sub-basin size. The log–log regression parameters and statistics for the eight stations appear to display variations with the size of sub-basin (Figure 8). In general, R^2 increases with size of the basin. This indicates a more pronounced relationship between sediment transport and river flow as one goes downstream.

Coefficient B is a measure of the rate at which hydrologic energy is converted to geomorphic work (Rannie, 1978; Mimikou, 1982). Coefficient B [Equation (1)] increases with the area of the basin (Figure 8). This implies that sediment concentration is more responsive to changing discharge for larger basins. This could occur if the proportion of basin affected by high erodibility and erosivity increase as one goes downstream.

Sub-basin sediment yields and basin parameters. The strength of the models (Figure 3) also suggests a sediment system that is not supply limited, since sediment concentration is closely coupled to flow. The

Table IV. Flow and sediment ratios at gauging stations

Station	River	Area (km^2)	Flow ratio[a]	Sed ratio[b]	Max.[c] monthly sed. transport (%)
Pejibaye	Pejibaye	128	64	236	6·10
Rivas	Chirripo	318	16	114	4·50
Las Juntas	Pacuar	323	27	162	3·30
Caracucho	Coto Brus	1133	16	97	3·10
La Cuesta	General	836	22	156	4·20
Remolino	General	1076	20	211	4·50
El Brujo	General	2401	20	249	6·00
Palmar	Terraba	4767	20	195	4·80

[a] Ratio of maximum daily to mean daily flow in 23 hydrologic years.
[b] Ratio of maximum daily sediment transport to mean daily transport (1971–93) estimated using parametric regression models.
[c] Maximum percentage of total cumulative sediment discharge over 23 years transported in a single month.

Sediment parameters
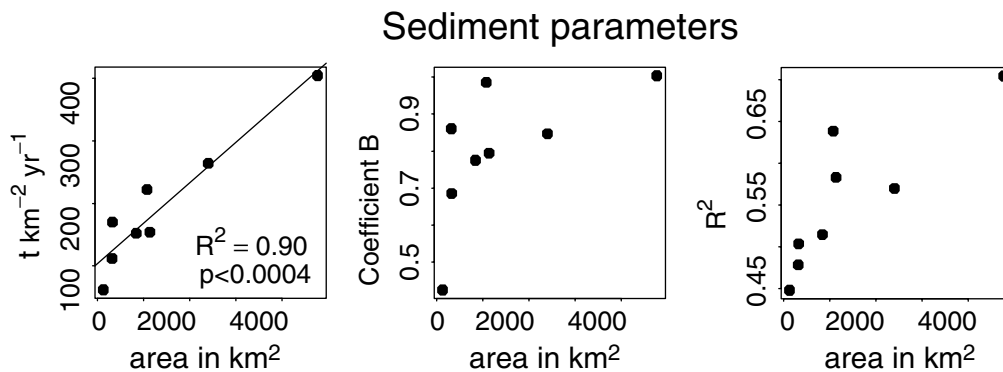
Figure 8. Trends in sediment model parameters with basin area. The first figure shows specific sediment yield as related to basin area. The second shows the relationship between the slope of the log–linear sediment–flow regression models (Figure 3) and the basin area for all the eight stations indicated in Figure 2. The third relates the R^2 for these regression models to the basin area for each of the gauging stations

association of R^2 and coefficient B with basin size is attributed to the increasing ability downstream of the watershed system to mobilize sediment from larger source areas without a reduction in sediment delivery ratios.

An analysis of basin factors was done to identify the most important factor in relation to observed trends in sediment yield downstream. Suspended sediment yields were positively related to area ($R^2 = 0.90$, $p < 0.0004$) and percentage area under agriculture ($R^2 = 0.63$, $p < 0.03$). Similar results were obtained for sediment yield estimates using the other three methods. Suspended sediment yields were significantly related to area (LOESS: $R^2 = 0.81$, $p < 0.003$, inst.sed: $R^2 = 0.85$, $p < 0.002$; piecewise-power: $R^2 = 0.44$, $p < 0.08$) and percentage area under agriculture (LOESS: $R^2 = 0.63$, $p < 0.02$, inst.sed: $R^2 = 0.75$, $p < 0.006$, piecewise-power: $R^2 = 0.58$, $p < 0.03$). This indicates that the results are not method specific. The other factors, such as slope, rainfall and percentage forest, were not significant in explaining the observed downstream trends in sediment yield. This suggests that the observed increase in specific sediment yield with basin area as one goes downstream is related to the pattern of land use, particularly the proportional increase in area under intensive agriculture.

The regression analyses of the larger data set for all of Costa Rica corroborated the results obtained for the Terraba basin. The intercept was removed whenever found non-significant. Sediment yield was significantly related to percentage area under agriculture ($n = 29$, $R^2 = 0.18$, $p < 0.05$). The best model to explain basin sediment yield was that with flow depth (flow per unit area) and percentage area under agriculture as independent variables ($R^2 = 0.64$, $p < 0.00001$, without intercept). The next best model was with flow depth and basin area ($n = 29$, $R^2 = 0.62$, $p < 0.00001$, without intercept). In general, in Costa Rica the larger basins tended to have higher sediment yields, because they are likely to have larger areas under agriculture, both in absolute and proportional terms.

The results from the regression approach applied to basin parameters suggest a strong association between land-use patterns and suspended sediment yields. In the following sections the spatial patterns of factors that affect erosion, and consequently sedimentation, will be investigated in detail.

Controls on erosion

The most important factors controlling erosion in the basin were identified as annual rainfall, rainfall erosivity, land use and slope. We discuss each of these in relation to the observed patterns of sediment yield.

Annual rainfall. The spatial pattern of annual rainfall in the basin (Figure 6) indicates that the highest rainfall (long-term mean) along the valley occurs in the northern part of the basin (>3600 mm) and decreases to less than 3000 mm as one goes downstream in a northwest to southeast direction towards the central part of

the basin. There is a relatively dry region in the central part. The rainfall again increases in the southeasterly direction and there is another wet region (3600–3900 mm) in the extreme southeast. The observed spatial gradient in rainfall is the opposite of the observed gradient in sediment yield along the Rio General River.

Rainfall erosivity. The erosivity map predicts high rainfall erosivity in the low and middle elevation regions, and in some very wet areas in the coastal range (Figure 6). An analysis of the rainfall–elevation relationship suggests that a simple orographic model of increasing rain with elevation cannot be applied in the Terraba basin (Krishnaswamy, 1999). The orographic effect is moderately expressed between 400 and 2000 m elevation, but above 2000 m there is a pronounced negative relationship. This implies that erosivity related to the wet-season intense showers (typically 1–6 h in late afternoon) is higher in the middle elevation region rather than in the high elevation region. Mikhailova *et al.* (1997) analysed the negative relationship between rainfall erosivity and elevation in some tropical and sub-tropical systems. At higher elevations, the low concentration of large drops formed by accretion and coalescence causes a decrease in raindrop mass, and this overcomes the influence of decreased air density on velocity. This results in a net decrease in the kinetic energy.

Based on erosivity alone, the most vulnerable areas for erosion in the Terraba basin would be the 500–2000 m elevation regions. Similar effects for other parts of Costa Rica have been noted by other researchers (Hastenrath, 1967; Mendizabal, 1973; Chacon and Fernandez, 1985). This would imply that rainfall erosivity increases as rivers and streams descend to the valley from the high mountains.

Slope. The trend of slope for the set of five nested stations from Rivas in the headwaters to Palmar at the basin mouth along the Rio General and Rio Terraba indicate that the distribution shifts towards lower values, although some very steep slopes flank the valley downstream nearer the basin mouth (Figure 9 and Table III). Some of these steep slopes are known to be unstable (Mora, 1989). The spatial distribution of slopes alone cannot account in large measure for the large increases observed in specific sediment yield between these nested stations. It is clear that other factors besides slope are at work.

Land use, erodibility, and erosion potential. Overall, the soils in the basin are well drained and less prone to erosion in their undisturbed state. The more weathered soils are less erodible than less weathered soils (Sanchez, 1976; El-Swaify and Dangler, 1982). In general, the more erodible soils, such as Inceptisols, occur in upper elevation areas with steep slopes and the less erodible soils, such as some Alfisols, Ultisols and Oxisols, occur on less steep slopes. Well-drained soils, such as Oxisols, that are relatively flat dominate the lower parts of the catchments; very steep slopes with unstable soils and channels dominate upper catchments positions. We do not attribute the observations of increase in sediment yield with area to be associated with geologic features. This implies that the increase in specific sediment yield with accumulation of lower elevation areas cannot be attributed to spatial patterns of native soil distribution. In fact, the opposite pattern would be expected. This suggests that other factors related to erodibility need to be considered.

As one goes down the main river to the basin mouth, there is a relative increase in the area under pasture and intensive agriculture (Figure 5). A large part of this area is under land-use practices that provide little protection against erosive rainfall (Figures 5 and 6).

We studied such conversion effects on older soils found on alluvial fans and terraces in the Rio General Valley of Costa Rica (Krishnaswamy, 1999). Soils on five interfluves that support forest and pasture were sampled to evaluate changes in physical and chemical properties to a depth of 120 cm. In addition, three of five blocks had plots under intensive agriculture. Soil carbon decreased in the surficial 30 cm by an estimated $15 \cdot 9_{median} \pm 10 \cdot 35_{95\%CI}$ Mg ha^{-1} after conversion. Forest conversion to pasture has increased mean surface (0–30 cm) bulk densities from 0·81 to 1·04 g cm^{-3} and decreased water-stable aggregates > 2 mm by 36·5%. Decreases in soil carbon were statistically ($R^2 = 0.34$, $p < 0.05$) associated with changes in percentage water-stable aggregates >0·25 mm. In areas with intensive agriculture, the losses of soil carbon are higher (32 Mg ha^{-1}), and the destabilization of soil aggregates, although not measured, is predicted to be even more pronounced.
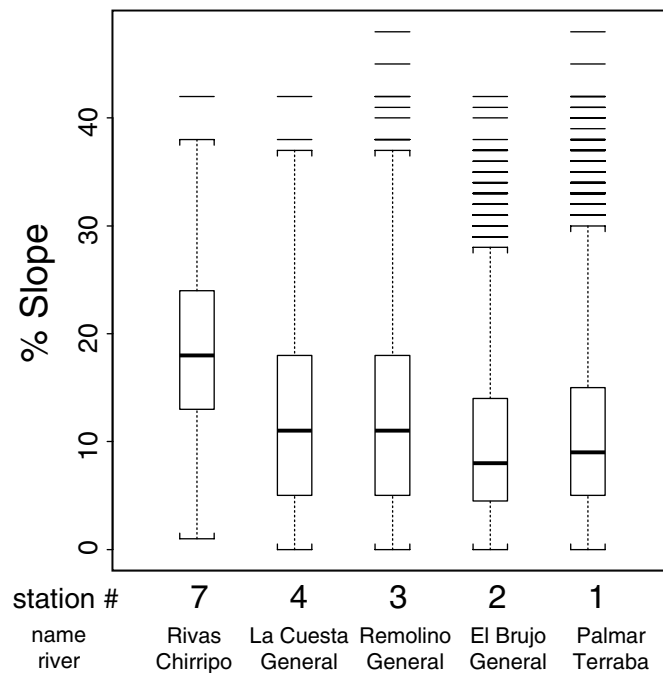
Figure 9. Trends in cumulative slope (%) downstream along nested stations numbered in Figure 2. The stations start from number 7, corresponding to a headwater sub-basin, to number 1 at the mouth of the basin

The consequences of these physical changes in the surficial soil layers for run-off generation, increased soil erosion and consequent sedimentation cannot be overstated.

Intensive sediment sampling during the wet season of 1995 demonstrated substantial spatial variability in sediment response to storms across the basin depending on land use and forest cover. Three of the eight sites correspond to sub-basins of comparable size but varied in their land use and topographic characteristics (Table V). The three basins represent a gradient of soil exposure. The highest sediment yields are obtained from areas under intensive agriculture.

Agricultural uses are most concentrated in the central and southern parts of the basin (Figure 5), and as one proceeds downstream there is an increase in area with erodible soils and exposure to high erosivity.

Two different erosion indices (Figure 10) derived for this study were used to compare the spatial distribution of predicted erosion. These indices integrate the most important determinants of erosion, rainfall erosivity, land use and slope. Erosion index 1, which was based on rainfall erosivity and land-use, reveals concentration of erosion in certain regions. The areas for which high erosion (>80 units or >8000 t km^{-2} year^{-1}) is predicted are concentrated in the central and southern parts of the basin, mainly in the intensive agricultural areas with

Table V. Sediment concentration in streams draining mixed land-use basins during 1995 wet-season storm sampling

Sub-basin	Area (km^2)	Elevation (msl)	Rainfall (mm)	Land-use/land-cover (%)				Sediment	concentration	quantiles
				forest	row-crops	agro-pasture	details	median	75%	95%
Guapinola	28	288–1060	2940	25	19	56	Pineapple	607	1405	2495
Quebradas	22	1100–2427	3300	29	0	71	Coffee, banana	227	473·5	2005
Canas	41	375–2763	3159	56	0	44	Pastures	21	21·75	43

high rainfall erosivity. These include: (1) the pineapple-growing areas on the river terraces and alluvial fans located between the Remolino and El Brujo gauging stations; (2) row-crops and pastures on deforested steep slopes in the coastal range, an area that drains to the Palmar station at the basin outlet.

The second erosion index includes slope in addition to land use and rainfall erosivity. This index predicts high erosion (>60 units or 20 000 t km^{-2} year^{-1}) for the unstable steep slopes exposed to high erosivity in parts of the southwestern coastal range, and for pasture and small row-crop fields on steep slopes (>20%) in the mid-elevation range of the Cordillera Talamanca. The intensive agricultural areas in the General valley have relatively lower predicted values (<30 units or 9000 t km^{-2} year^{-1}), whereas predicted erosion for high elevation forests and lower elevation pastures are very low (<20 or 7200 t km^{-2} year^{-1}).

The two indices were used to compare their performances in explaining the observed increase in specific sediment yield from upstream to downstream. The mean cumulative erosion from the two erosion indices was plotted against basin area as gauged at each of five stations (stations 7, 4, 3, 2 and 1 in Figure 2). The specific sediment yield normalized to a similar scale was also plotted. The results (Figure 10) indicate that
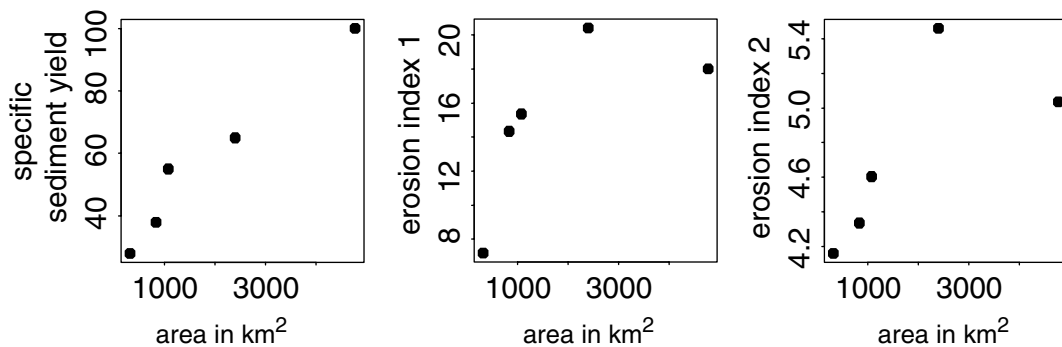
Figure 10. Trends of erosion indices (see Figure 7) with basin area. The erosion index value for a sub-basin was calculated by taking the average of all the pixel values corresponding to the upstream sub-basin for each station
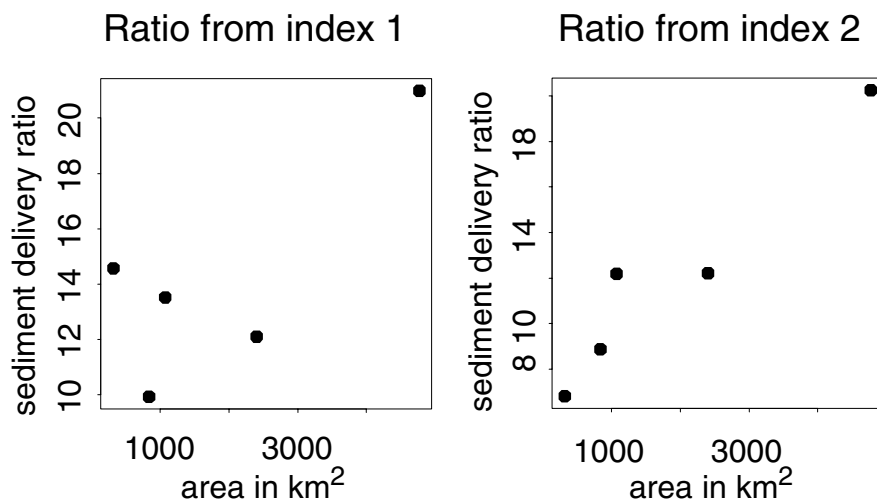
Figure 11. Trends in estimated hill-slope SDRs with basin area along nested stations. The SDR was estimated by taking the ratio of sediment yield data from the eight stations to the estimated USLE erosion values for sub-basins corresponding to these stations. USLE estimates for three sub-basins were available, and these were used to calibrate the erosion indices to USLE-based actual erosion units for the remaining five stations as well

the pattern of cumulative erosion as predicted by both the indices are very similar to the observed increase in specific sediment yield from La Cuesta to El Brujo on the Rio General. It is interesting to note that the highest cumulative erosion index values belong to the El Brujo station, just downstream of intensive agricultural and degraded areas, and the highest specific sediment yield from the ICE Piece-wise power method is also for this station, although the other three methods differ in this respect (Table III). Estimated sediment delivery ratios (SDR) also increase downstream, especially for erosion index 2 (Figure 11). This is attributed largely to contributions from very steep unstable slopes near the basin mouth (Figures 9 and 10). In addition, the spatial distribution of intensive land use, mainly agriculture, and its exposure to high erosivity rainfall leads to an increase in sediment source areas along the Rio General.

The combination of an increase in erodible disturbed soils exposed to high erosivity rainfall and a high SDR would explain the observed pattern of increasing specific sediment yield with basin area. Eroded soil appears to be transformed to stream sediment and flushed through the stream system with supply far exceeding storage in channel reaches.

CONCLUSION

The Terraba basin is a good example of a disturbed, heterogeneous tropical basin with considerable spatial variability of sediment yield. This variability is linked primarily to spatial patterns of land-use disturbance and rainfall erosivity. As a consequence of both land-use patterns and the spatial distribution of rainfall erosivity, especially in relation to location of natural instabilities, the trends of sediment parameters with respect to basin size are contrary to what is usually assumed. The specific sediment yield estimated for nested stations increased from 152 ± 33.9 t km^{-2} year^{-1} at 836 km^2 to 404 ± 141.7 t km^{-2} year^{-1} at 4767 km^2 at the basin mouth. Topography appears to be less influential overall, except in a few unstable areas with high rainfall erosivity. This is because the steep slopes are better protected. The downstream pattern of SDR in combination with increased opportunities of erosion explains the observed increase in specific sediment yield with basin area. This study illustrates the utility of a rigorous quantitative–analytical framework within which complex basin processes can be studied.

This study indicates that improvements in land use and soil management in the Terraba basin should be concentrated on lower-lying alluvial fans, especially in fields intensively managed for agricultural crops. Naturally unstable areas should be monitored carefully and protective land use promoted. Sustaining current and future land uses would benefit from better management of surficial organic matter, which controls nutrient retention and soil structural stability in these soils. The acceleration of erosion by intensive agriculture should be a cause of concern because of the loss and degradation of soil and water resources.

REFERENCES

Ashmore P. 1992. Sediment delivery in large prairie river basins, western Canada. *International Association of Hydrological Sciences Publication* **210**: 423–432.

Bobrovitskaya NN, Zubkova CM. 1998. Application of formulae of transporting flow capacity for the computation of suspended in the Lena river. *International Association of Hydrological Sciences Publication* **249**: 149–156.

Boucher DH, Hansen M, Risch S, Vandermeer JH. 1983. Agriculture. In *Costa Rican Natural History*, Janzen D (ed.). The University of Chicago Press: Chicago, IL; 66–77.

Bruijnzeel LA. 1990. *The Hydrology of Moist Tropical Forest and Effects of Conversion: A State of Knowledge Review*. International Association of Hydrology. UNESCO, Paris and Free University: Amsterdam, The Netherlands.

Bruijnzeel LA. 1993. Land–use and hydrology in warm humid regions: where do we stand? *International Association of Hydrology Publication* **216**: 3–34.

Bull LJ, Lawler DM, Leeks GJL, Marks S. 1995. Downstream changes in suspended–sediment fluxes in the River Severn, UK. *International Association of Hydrology Publication* **226**: 27–38.

Calvo J. 1998. Suspended sediment yield prediction models for Costa Rican watersheds. *International Association of Hydrologic Sciences Publication* **253**: 27–32.

Castillo-Munoz R. 1983. Geology. In *Costa Rican Natural History*, Janzen D (ed.). The University of Chicago Press: Chicago, IL; 47–62.

Chacon RE, Fernandez W. 1985. Temporal and spatial rainfall variation in the mountainous region of the Reventazon River Basin, Costa Rica. *Journal of Climatology* **5**: 175–188.

Clarke RT. 1990. Statistical characteristics of some estimators of sediment and nutrient loadings. *Water Resources Research* **26**: 2229–2233.

Cleveland WS. 1979. Robust locally weighted regression and smoothing scatterplots. *Journal of American Statistical Association* **74**: 829–836.

Cleveland WS, Devlin SJ. 1988. Locally-weighted regression: an approach to regression analysis by local fitting. *Journal of American Statistical Association* **83**: 596–610.

Cohn TA, Caulder DL, Gilroy EJ, Zynjuk LD, Summers RM. 1992. The validity of a simple statistical model for estimating fluvial constituent loads: an empirical study involving nutrient loads entering Chesapeake bay. *Water Resources Research* **28**: 2353–2363.

Dedkov AP, Moszherin VT. 1992. Erosion and sediment yield in mountain areas of the world. *International Association of Hydrological Sciences Publication* **209**: 29–36.

Dickinson A, Bolton P. 1992. A program of monitoring sediment transport in north central Luzon, Philippines. *International Association of Hydrological Sciences Publication* **210**: 483–492.

Dunne T. 1979. Sediment yield and land-use in tropical catchments. *Journal of Hydrology* **42**: 281–300.

Dunne T, Dietrich W. 1982. Sediment sources in tropical drainage basins. In *Soil Erosion and Conservation in the Tropics*, ASA Special Publication no. 43. Soil Science Society of America: Madison, WI; 41–56.

El-Swaify SA. 1990. Research needs and applications to reduce erosion and sedimentation in the tropics. *International Association of Hydrological Sciences Publication* **192**: 3–13.

El-Swaify SA, Dangler EW. 1977. Erodibilities of selected tropical soils in relation to structural and hydrological parameters. *Soil Conservation Society of America Special Publication* **21**: 105–115.

El-Swaify SA, Dangler EW. 1982. Rainfall erosion in the tropics: a state of the art. In *Soil Erosion and Conservation in the Tropics*, ASA Special Publication no. 43. Soil Science Society of America: Madison, WI; 1–25.

Ferguson RI. 1986. River loads underestimated by rating curves. *Water Resources Research* **22**: 74–76.

Guy HP, Norman VW. 1970. Field measurements for measurement of fluvial sediment. *USGS–TWRI Book 3*. US Geological Survey: Denver, CO; chapter C2.

Hastenrath S. 1967. Rainfall distribution and regime in central America. *Archiv Meterologie, Geophysik und Bioklimatologie, Serie B: Klimatologie, Umweltmeterologie, Strahlungsforschung* **15**: 201–241.

ICE (Instituto Costarricense de Electricidad). 1973. Informe Hidrologico Proyecto Boruca. San Jose, Costa Rica.

ICE (Instituto Costarricense de Electricidad). 1994a. Precipitacion pluvial mensual. Systema Hidromet. San Jose, Costa Rica.

ICE (Instituto Costarricense de Electricidad). 1994b. Registro de caudales. Medios diarios. Departmento de hidrologia-oficina Hydrologia operativa. Direccion de planification electrica. San Jose, Costa Rica.

IMN (Instituto Meterolologico Nacional). 1988. Catastro de las series de precipitaciones medidas en Costa Rica MIRENEM. San Jose, Costa Rica.

Jansson MB. 1988. A global survey of sediment yield. *Geografiska Annaler, Series A* **70A**(1–2): 81–98.

Kesel RH, Spicer BE. 1985. Geomorphologic relationships and ages of soils on alluvial fans in the Rio General valley, Costa Rica. *Catena* **12**: 149–166.

Kithiia SM. 1997. Land use changes and their effects on sediment transport and soil erosion within the Athi drainage basin, Kenya. *International Association of Hydrological Sciences Publication* **245**: 145–150.

Koch RW, Smillie GM. 1986. Comment on "River loads underestimated by rating curves" by R.I. Ferguson. *Water Resources Research* **22**: 2121–2122.

Krishnaswamy J. 1999. Effects of forest conversion on soil and hydrologic processes in the Terraba basin of Costa Rica. PhD thesis, Duke University, USA.

Lal R. 1977. Analysis of factors affecting rainfall erosivity and soil erodibility. In *Soil Conservation and Management in the Humid Tropics* Greenland DJ, Lal R (eds). Wiley: New York; 49–56.

Lal R, Lawson TL, Anastase AH. 1980. In *Erosivity of Tropical Rains. Assessment of Erosion*. Wiley: New York; 143–151.

Larsen MC. 1997. Tropical geomorphology and geomorphic work: a study of geomorphic processes and sediment and water budgets in montane humid-tropical forested and developed watersheds, Puerto Rico. Unpublished PhD thesis, University of Colorado Geography Department; 341 pp.

MAG. 1991. Manual descriptiva de la leyenda del Mapa de capacidad de uso de la tierra de Costa Rica. Ministerio de agricultura y ganaderia, San Jose, Costa Rica.

Meade RH. 1982. Sources, sinks and storage of river sediment in the Atlantic drainage of the United States. *The Journal of Geology* **90**: 235–252.

Mendizabal M. 1973. Distribucion de la precipitacion con altura. Ciudad Universitaria: Escuela de fisica, Universidad de Costa Rica.

Mikhailova EA, Bryant RB, Schwager SJ, Smith SD. 1997. Predicting rainfall erosivity in Honduras. *Soil Science Society of America Journal* **61**: 273–279.

Mimikou M. 1982. An investigation of suspended sediment rating curves in western and northern Greece. *Hydrological Sciences* **27**: 369–383.

MIRENEM. 1988. Mapa de Cobertura Boscosa de Costa Rica (+60% densidad, scale 1:200 000). Ministerio de Recursos Naturales, Energia y Minas, Direccion General Forestal: San Jose, Costa Rica.

Mora SC. 1989. Extent and social–economic significance of slope instability in Costa Rica. In *Landslides: Extent and Economic Significance*. Proceedings of the 28th International Geological Congress: Symposium on Landslides. Balkema: Rotterdam; 93–99.

Pachon C. 1996. Land use impacts on surface water resources in a humid, tropical basin. Master's project, Nicholas School of the Environment, Duke University, Durham, NC.

Parker RS, Troutman BM. 1989. Frequency distribution for suspended sediment loads. *Water Resources Research* **25**: 1567–1574.

Rannie WF. 1978. An approach to the prediction of sediment-rating curves. In *Research in Fluvial Systems*. Davidson-Arnott R, Nickiling W (eds). Geobooks: Norwich, UK.

Sader S, Joyce AT. 1988. Deforestation rates and trends in Costa Rica, 1940 to 1983. *Biotropica* **20**: 11–19.

Sanchez PA. 1976. *Properties and Management of Soils in the Tropics*. Wiley: New York.

Simon A, Guzman-Rios S. 1990. Sediment discharge from a montane basin, Puerto Rico: implications of erosion processes and rates in the humid tropics. In *Research Needs and Applications to Reduce Erosion and Sedimentation in Tropical Steeplands*. International Association of Hydrological Sciences Publication **192**: 35–47.

Sivapalan M, Kalma JD. 1995. Scale problems in hydrology: contributions of the Robertson workshop. *Hydrological Processes* **9**: 243–250.

Skutch AF. 1971. *A Naturalist in Costa Rica*. University of Florida Press: Gainesville, FL.

Soto WHR, Gomez LDP. 1993. Mapa de Unidades Bioticas de Costa Rica. INCAFO, S.A.: San Jose, Costa Rica.

USGS. 1997. United States Geological Survey. GTOPO30 Global 30 Arc Second Elevation Data Set. http://edcwww.cr.usgs.gov/landdaac/gtopo30/gtopo30.html

Vahrson W. 1990. El potencial erosivo de la lluvia en Costa Rica. *Agronomia Costarricense* **14**: 15–24.

Walling DE. 1983. The sediment delivery problem. *Journal of Hydrology* **65**: 209–237.

Williams D. 1995. A spatial analysis of the controlling factors of suspended sediment yield in Costa Rican rivers. Master's Project, Nicholas School of the Environment, Duke University, Durham, NC.

Wolman MG, Schick AP. 1967. Effects of construction on fluvial sediment: urban and suburban areas of Maryland. *Water Resources Research* **6**: 1312–1326.